Published in final edited form as:

J Biomed Mater Res A. 2018 February ; 106(2): 450–459. doi:10.1002/jbm.a.36235.

Nerve-Specific, Xenogeneic Extracellular Matrix Hydrogel Promotes Recovery Following Peripheral Nerve Injury:

Peripheral Nerve-Specific Extracellular Matrix Hydrogel

Travis A. Prest, BS[1,2], **Eric Yeager, MS**[3], **Samuel T. LoPresti, BS**[1,2], **Emilija Zygelyte, BS**[3], **Matthew J. Martin, BA**[3], **Longying Dong, PhD**[3], **Alexis Gibson**[3], **Oluyinka O. Olutoye**[1,2], **Bryan N. Brown, PhD**[1,2,3,*], and **Jonathan Cheetham, VetMB, DACVS, PhD**[1,3,*]

[1]McGowan Institute for Regenerative Medicine, University of Pittsburgh, Pittsburgh, PA

[2]Department of Bioengineering, University of Pittsburgh, Pittsburgh, PA

[3]Department of Clinical Sciences, Cornell University, Ithaca, NY

Abstract

Peripheral nerve possesses the inherent ability to regrow and recover following injury. However, nerve regeneration is often slow and incomplete due to limitations associated with the local microenvironment during the repair process. Manipulation of the local microenvironment at the site of nerve repair, therefore, represents a significant opportunity for improvement in downstream outcomes. Macrophages and Schwann cells play a key role in the orchestration of early events after peripheral nerve injury. We describe the production, characterization, and use of an injectable, peripheral nerve-specific extracellular matrix-based hydrogel (PNSECM) for promoting modulation of the local macrophage and Schwann cell responses at the site of nerve repair in a rodent model of sciatic nerve injury. We show that PNSECM hydrogels largely maintain the matrix structure associated with normal native peripheral nerve tissue. PNSECM hydrogels were also found to promote increased macrophage invasion, higher percentages of M2 macrophages and enhanced Schwann cell migration when used as a lumen filler in a rodent model of nerve gap repair using an inert nerve guidance conduit. These results suggest that an injectable PNSECM hydrogel can provide a supportive, bioactive scaffold which promotes repair of peripheral nerve *in vivo.*

Keywords

Nerve; regenerative medicine; extracellular matrix; hydrogel; macrophage

INTRODUCTION

Despite advances in microsurgical technique and extensive studies on nerve repair, presently used surgical re-innervation methods produce only moderate results and full functional

*Corresponding Authors: Bryan N. Brown, Suite 300, 450 Technology Drive, Pittsburgh, PA 15218, P:(412) 624-5273, F:(412) 624-5363, brownb@upmc.edu, Jonathan Cheetham, Box 34, College of Veterinary Medicine Ithaca, NY 14850 P:(607) 253-3100 F: (607) 253-3271, jc485@cornell.edu.

recovery after nerve injury is seldom achieved. [1–4] Therefore, methods that accelerate or improve re-innervation following reconstruction of peripheral nerve are of significant clinical interest. One opportunity for functional improvement after nerve reconstruction or grafting is manipulation of the microenvironment at the site of nerve repair to promote modulation of the host inflammatory response and to promote Schwann cell migration and axon extension across the repair site. [5–8] Extended axonal regrowth cannot occur without closely apposed Schwann cells (SC) [9] and the specificity of this process is enhanced both by extracellular matrix (ECM) components, such as collagen IV or laminin, which provide basement membrane support for SC migration and by neovascularization promoted by certain macrophage subsets. [5,9–13] Macrophages are a key component of the host response to nerve injury [5] and have been described as having diverse and plastic phenotypes along a continuum between M1 (classically activated; proinflammatory) and M2 (alternatively activated; remodeling, homeostatic) extremes. [14–16] M1 macrophages are characterized by the secretion of reactive oxygen species and proinflammatory cytokines and chemokines. Persistence of M1 macrophages can lead to tissue damage and destruction. In contrast, M2 macrophages secrete anti-inflammatory immune modulators and participate in the constructive healing and remodeling phase of the tissue remodeling response by promoting tissue deposition and in growth.

Numerous approaches for delivery of matrix components, immunomodulatory or growth factors, and cells to the site of nerve repair have been used. The majority of studies have investigated single or combinations of a small number of additives to common hollow tube nerve guidance conduits with the goal of altering the local environment and improving recovery through the addition of growth factors such as Brain Derived Neurotrophic Factor (BDNF), Glial Derived Neurotrophic Factor (GDNF), Nerve Growth Factor (NGF), Neurotrophibn-3 (NT-3) or accessory cells into a supportive matrix (Table 1). [17–29] While many of these studies have reported positive outcomes, limitations include tailoring growth factor release profiles, optimizing the mechanical environment of the substrate used at the site of repair, and maintaining cell viability after transfer. [18,30] One alternative to engineering a complex microenvironment is to mimic the native microenvironment of healthy peripheral nerve using a decellularized tissue based hydrogel.

Scaffolds composed of extracellular matrix (ECM) derived through the decellularization of intact tissues and organs have been shown to promote a process of “constructive remodeling” following injury, [31] including the formation of new, functionally innervated, site-appropriate host tissue. [32–34] While the exact mechanisms which underlie the ability of these materials to promote such remodeling are unknown, a number of studies have now shown that the release of bioactive tissue specific molecules and a shift in the local inflammatory response at the site of implantation are key occurrences during the remodeling process. [31] A number of ECM scaffolds have been demonstrated to be supportive substrates for axonal growth and the degradation products of such materials have been demonstrated to be bioactive and chemotactic for SC. [32,35,36] Recently, a method for fabricating ECM scaffold degradation products into injectable, temperature responsive, hydrogels has been described, [36,37] enabling delivery in multiple settings without prior fabrication of solid matrices into specific shapes and sizes.

Here we describe the generation and characterization of an injectable, peripheral nerve-specific extracellular matrix-based (PNSECM) hydrogel for peripheral nerve repair. We then test the effects of these hydrogels in a classical rodent nerve injury model to assess their potential for use in nerve repair. Specifically, we focus upon two key early events in the remodeling process: modulation of the host macrophage response and recruitment of Schwann cells. We then evaluate the effects of PNSECM on functional recovery in a rodent nerve gap defect model.

MATERIALS AND METHODS

Preparation of Peripheral Nerve ECM

Canine sciatic nerves were harvested following euthanasia of adult animals for reasons unrelated to nerve injury or neurological disease. The tissue was then frozen for at least 16h at −80°C. The outer portion of the epineurium of the nerve was stripped by sharp dissection and mechanical delamination, leaving the nerve bundles intact. The tissue was then sectioned longitudinally and cut into lengths of < 5cm and quartered lengthwise prior to treatment.

Tissues were then processed using a modification of a protocol for spinal cord de-cellularization as previously described. [38]

Briefly, the decellularization process consisted of a series of agitated washes: water (type 1, ultrapure, Milli-Q® purified water,14 hours at 4°C), 0.02% trypsin (HyClone) /0.05% EDTA (Invitrogen, Waltham, MA USA) (60 minutes at 37°C), 3.0% Triton X-100 (Sigma, 60 min), water rinse (type 1, repeated until agitation no longer produced bubbles), 1M sucrose (Thermo Fisher, Waltham, MA USA, 15 min), 4.0% sodium deoxycholate (Sigma, St. Louis, MO, USA 60 min), 0.1% peracetic acid/4% ethanol (Sigma, 120 min), 1X PBS (15 min), water (14 hours), 1X PBS (15 min). Following treatment, samples were frozen (-80°C) and then lyophilized.

The present studies utilized urinary bladder matrix from a canine source as a control for characterization of decellularization and biochemical composition. Urinary bladder matrix was chosen as a control as it is a well characterized source for tissue decellularization, protocols resulting in effective decellularization have been established. Canine urinary bladder matrix was prepared as previously described. [39] Briefly, the tissue was bisected into a sheet and mechanically delaminated to remove the outer muscular layers, leaving the urothelial basement membrane and underlying connective tissue intact. The delaminated tissue was then subjected to washes in 0.1% peracetic acid/4% ethanol (Sigma, 120 min), 1X PBS (15 min), water (14 hours), 1X PBS (15 min). All tissues were then treated in a manner similar to that described for PNSECM.

Confirmation of Decellularization

Qualitative assessment of cellular content was performed using histologic staining and immunofluorescent labeling. Fixation of lyophilized ECM scaffolds was performed in 10% neutral buffered formalin (Electron Microscopy Sciences, Hatfield, PA, USA). Samples were embedded in paraffin, sectioned, and stained with hematoxylin and eosin (H&E) or with 4',

6-diamidino-2-phenylindole DAPI to verify removal of nuclei. Additional samples were stained using Luxol fast blue to determine removal of myelin as an additional metric of decellularization. Qualitative assessment of DNA content was conducted by digesting the ECM scaffold in 0.1 mg/mL proteinase K solution (Invitrogen). Protein content was removed from the sample by repeated phenol/chloroform/isoamyl alcohol (Thermo Scientific) extraction and centrifugation (10,000 G) until no protein precipitate was observed at the interface. The aqueous layer was mixed with 3 M sodium acetate (Fisher Scientific) and 100 % ethanol. The solution was frozen using dried ice and centrifuged to produce a DNA pellet. The pellet was rinsed with 70% ethanol, centrifuged (10,000 G), and dried. Double-stranded DNA was then quantified using Quant-iT™ PicoGreen dsDNA assay kit (Life Technologies) following kit instructions. Statistical significance was assessed using one-way ANOVA with Tukey post-hoc test. Additionally, agarose gel electrophoresis was performed to assess base pair length of any remaining DNA.

Assessment of Extracellular Matrix Ultrastructure and Components

Maintenance of collagen IV, an extracellular matrix component of the basal lamina was assessed using immunolabeling. Scaffold materials were fixed in 10% neutral buffered formalin, embedded in paraffin and sectioned at 5 μm. Immunolabeling was performed with antibodies specific to ECM components (collagen I, III, and IV). Briefly, after deparaffinization, all slides were subjected to antigen retrieval by immersion in 95°C–100°C in citric acid solution (Acros Organics, Waltham, MA USA, 10 mM, pH 6.0; 20 min), followed by rinsing in a 1X Tris buffered saline/Tween-20 solution (0.1% Tween 20, Fisher Scientific, v/v, pH 7.4; 3 washes, 5 minutes each). Samples were then washed in PBS and treated with a pepsin digestion (0.05% pepsin, Sigma, w/v in 10 mM HCl, 15 minutes at 37°C) solution for further antigen retrieval. Samples were blocked against nonspecific binding using a solution consisting of 2% horse serum, 1% bovine serum albumin, 0.1% Tween-20, and 0.1% Triton X-100 in PBS for 30 minutes at room temperature. Primary antibodies for collagen I, III, and IV (Sigma, 1:200) were applied to sections overnight at 4°C. Samples were washed in PBS and appropriate fluorescently labeled secondary antibodies (AlexaFluor 488, 1:250) were applied for 60 minutes at room temperature.

For scanning electron microscopy (SEM), lyophilized samples were fixed in cold 2.5% (v/v) glutaraldehyde and processed using a standard SEM preparation procedure. The dried samples were mounted onto aluminum stubs and sputter coated with a 3.5 nm layer of gold–palladium alloy prior to imaging. Quantitative assessment of collagen (hydroxyproline) and glycosaminoglycan (GAG) content was performed through spectrophotometric assays. 100 mg of dry tissue was digested overnight at 60°C in 0.125 mg/ml papain (Sigma) in phosphate buffer with 0.01 M EDTA and 0.01 M cysteine (Sigma). Afterwards, GAG content was assessed by mixing aliquots of the resultant digest with the dye 1,9-dimethylmethylene blue (Fisher Scientific) and reading the absorption of a 525 nm wavelength. Hydroxyproline content was analyzed as per a published protocol. [24] Statistics for both assays were calculated using one-way ANOVA with a Tukey post-hoc test.

Formation of hydrogel from enzymatic degradation products

Enzymatic degradation products were generated from PNSECM scaffold materials as previously described. [36]

Briefly, lyophilized scaffold materials were powdered and solubilized at a concentration of 20 mg/mL in a solution containing 2.0 mg/mL pepsin (Sigma) in 0.01 N HCl (ACROS organic) at a constant stir rate for 48h. The resultant ECM digest solution was then frozen at −80°C until use in subsequent experiments. ECM hydrogels were formed from the degradation products as previously described. [36] Briefly, gelation was induced by adjusting the pH of the pepsin digest to 7.4 through the addition of one-tenth the digest volume of 0.1 M NaOH, one-ninth the digest volume of 10X PBS, and then diluting to the desired final ECM concentration in 1X PBS. Dilutions were performed on ice and the gel solution was placed in a non-humidified incubator at 37°C and allowed to gel for 1h for benchtop confirmation of gelation. Concentrations between 8 and 15 mg/mL were examined visually for their ability to form a hydrogel. Hydrogels were prepared and evaluated under SEM using a standard preparation procedure and imaged at 4,000 magnification..

Ethics Statement

Animal studies were performed in accordance with the PHS Policy on Humane Care and Use of Laboratory Animals, the NIH guide for Care and Use of Laboratory Animals, federal and state regulations, and was approved by the Cornell University Institutional Animal Care and Use Committee (IACUC). Animals were brought into the research unit and given a 7-day acclimatization period prior to any procedure. Daily record logs of medical procedures were maintained. Cages with elevated floors were cleaned daily and disinfected biweekly. ARRIVE guidelines for reporting *in vivo* experiments were used throughout. [40]

Assessment of Macrophage Response and Schwann Cell Migration

To determine the effects of cell PNSECM on macrophage and Schwann cell migration animals underwent creation of a sciatic nerve gap defect followed by repair with a silicone conduit alone (n=7) or a silicone conduit with PNSECM (n=7). Rats (Sprague Dawley, females, 200–250g) were pre-medicated with subcutaneous buprenorphine (2mg/kg), anesthetized with isoflurane and maintained under anesthesia with isoflurane/oxygen. The sciatic nerve was exposed and transected and a 15mm critical-length defect [41] was created within a 17 mm silicone nerve conduit (Tuzic, Siliclear tubing, 4.6mm OD, 3.4mm ID). Proximal and distal nerve stumps were aligned and sutured 1mm into the conduit with 9-0 suture. Conduits were filled with PNSECM hydrogel at a concentration of 8 mg/ml, prepared as described above. The hydrogel was brought to room temperature 5 minutes prior to injection into the conduit. The hydrogel was observed to gel within the silicone conduit with 5 minutes. Excess gel was removed and the site irrigated with saline solution. Muscular and cutaneous layers were closed routinely. Post-surgical pain control was provided by subcutaneous meloxicam (2mg/kg) injection immediately postoperatively and 12 hours after surgery. Rats were euthanized with pentobarbital (I.P.) 21 days after implantation and the conduit and proximal and distal stumps removed intact. Samples were fixed in Zamboni's solution for immunofluorescent labeling as described below.

Immunolabeling and Quantitative Analysis

Samples were embedded in paraffin and sectioned longitudinally at 4 μm for immunofluorescent labeling to assess the host macrophage, and Schwann cell response. Complete consecutive sections were used for M1, M2 and Schwann cell labeling. Three slides from each rat were generated for each label. After deparaffinization and rehydration, antigen retrieval was performed by steaming in 10 mM citrate (pH 6.0) for 20 min followed by incubation for 20 min at room temperature. Sections were then processed with a MicroProbe System (Fisher Scientific) and phosphate buffered saline containing 0.05% Tween 20 (PBST) was used for washing between each of the steps described below. Slides were blocked in a solution of 2x casein and 10% antibody host species matched serum for 30 minutes at room temperature. The sections were then incubated with a mixture of antibodies specific for markers of M1 macrophages (CD68, CCR7), M2 macrophages (CD68, CD206), and Schwann cells (GFAP) for 90 minutes at room temperature. Incubation in appropriate AlexaFluor 488 and Texas Red conjugated secondary antibodies was performed sequentially for 30 minutes each at room temperature. Sections were coverslipped in an aqueous mounting media containing DAPI (Vectashield, Vector Laboratories). For negative control, the primary antibodies were replaced with a mixture of isotype IgG at equivalent concentrations. Antibody species, isotype, dilution, and supplier information are provided in Table 2.

High resolution images of the entire proximal stump and regenerative bridge were obtained from fluorescently labeled slides (Zeiss 510). The original site of transection was identified in each image and a straight line drawn perpendicular to the long axis of the nerve at that level to allow identification of individual cells relative to this line (Volocity Image Analysis Software, Perkin Elmer). The location of all individual macrophages (M1, CD68+ CCR7+; or M2, CD68+ CD206+) and Schwann cells (GFAP+) and their location relative and perpendicular to the transected proximal nerve stump were then determined (Volocity) with concealment of group allocation. Cell position (M1, M2 macrophage or Schwann cell) relative to the original site of transection was binned into 500μm increments, log transformed and treated as a categorical variable to allow for non-linear effects. M2:M1 ratio was calculated for each section as the total number of CD68/CD206+ macrophages divided by the total number of CD68/CCR7+ macrophages. The distribution of each cell population was analyzed using a mixed effect models, with animal identity as a random effect. Linear contrasts were used to make specific comparisons when appropriate.

Functional Assessment in rodent gap defect using walking track analysis

To evaluate the effects of PSECM on functional recovery, a non-critical 8mm gap defect was created in the common peroneal nerve using a 10mm conduit in the left hind limb of Sprague Dawley rats (females, 200–250g). Conduits were filled with PNSECM or left empty (control, n=6 /group). All surgeries were block randomized and anesthetic and surgical procedures were performed as described above. Walking track analysis was used to determine hind limb function using a modified peroneal functional index (PFI) before injury (week 0) and 2, 4, 8, 12 and 16 weeks after repair[42]. Briefly, a minimum of three walking track assessments were obtained by inking the rat's feet, using an oversized inking pad (Ranger Industries, Tinton, NJ), and then permitting them to run across a single 43 cm long

by 10 cm wide piece of plain white paper within a clear Perspex corridor. Three trials for each rat at each time point were retained for analysis, and rejection of a trial occurred if the rat paused or stopped in the middle of the trial or otherwise did not maintain a relatively constant velocity or if the prints made were unusable due to poor inking. Walking tracks were scanned into digital images (CanoScan LiDE 110, Canon USA, Inc, Melville, NY), and measurements for print length (PL, the distance between cranial extent of digit III and caudal extent of the print); total spread (TS, the distance between the centers of paw pad I and paw pad V); intermediate toe spread (IT, the distance between the centers of paw pad II and paw pad IV); distance to the opposite foot (TOF, the vertical distance between the cranial aspects of contralateral prints) and deviation angle (DA, the angle of the foot with respect to the direction of travel; destination = 180°) obtained, with concealment of group allocation, using Photoshop CS6® software (Adobe Systems, Inc., San Jose, CA). All measurements for all prints were recorded for each trial (usually 2 prints per limb) and mean measurements determined from all ipsilateral prints.

Factors contributing to PFI (PL, IT and DA) were calculated as a percentage of baseline (preinjury) value rather than as a percentage of the contralateral limb. Modified PFI was calculated as PFI= $(-55.47\times PL)+(74.87\times IT)+(163.43\times DA)-2.18$. A mixed effect model was fitted to the data with animal identity as a random effect. Time after injury (weeks) was treated as a categorical variable to allow for a non-linear effect of time and an interaction term (time*group) included. Tukey's post hoc tests and linear contrasts were used as appropriate. Statistical analysis was performed using one-way ANOVA and Tukey post-hoc with SPSS (IBM Corporation, Armonk, NY, USA) or JMP (SAS Institute, Cary, North Carolina, USA). Significance was set at $p<0.05$ throughout.

RESULTS

Confirmation of Decellularization

Following decellularization of canine sciatic nerve, few nuclei were visible in hematoxylin and eosin (H&E) stained sections under light microscopy (Figure 1A–B). In some samples, a small number of nuclei (5–10 nuclei/20X field) were observed when labeled with DAPI (Figure 1C–D). When present, retained nuclei were observed within the central most nerve fascicles relative to the whole nerve tissue or within the dense perineurium of the treated tissues. Myelin, a potentially immunogenic axonal component, [43] was reduced after decellularization process (Figure 1E–F).

dsDNA content was decreased by approximately 85% in the decellularized tissue (158.1 ± 34.5 ng/mg) compared to native tissue (1,043.6 ± 291.2 ng/mg) (Figure 1G). These values are consistent with those reported for multiple FDA approved, commercially available ECM scaffold materials. [44]

Maintenance of Extracellular Matrix Ultrastructure and Components

Maintenance of the basal lamina was investigated through staining of collagen IV, a major constituent of the basal lamina. While immunofluorescent labeling showed that the content and organization of collagen I and III was affected by decellularization (Figure 2A–D),

collagen IV within individual nerve bundles was strongly preserved (Figure 2E–F). Strong positive staining within the decellularized samples both within the endoneurial basal lamina and within the perineurium (Figure 2E–F), suggests a strongly preserved basal lamina structure. The intensity of the staining within the endoneurium, however, was less than the perineurium and the architecture was slightly disrupted as compared to native tissue.

Biochemical testing was performed to assess the quantity of basic ECM components including hydroxyproline and glycosaminglycans (GAG). Hydroxyproline concentration within the scaffold material was unchanged by decellularization ($p = 0.57$). PNSECM contained less hydroxyproline than UBM ($p = 0.001$) (Figure 2K). GAG content decreased slightly after decellularization but not significantly ($p = 0.26$) and still contained more than UBM ($p=0.001$, Figure 2L).

The solubilized PNSECM can be reconstituted into a stable hydrogel at concentrations as low as 8 mg/ml. This was visually confirmed by depositing the neutralized PNSECM solution within a stainless steel ring and incubating at 37°C for 30 min (Figure 2M). Under SEM, the hydrogel was characterized by a highly porous network of fibular proteins (Figure 2N).

Assessment of Macrophage Response and Schwann Cell Migration

Macrophage phenotype—Macrophages within the remodeling site tended to be distributed on the margins of the regenerative bridge (Figure 3) and the number of both M1 and M2 macrophages (M1: CD68+ CCR7+; M2: CD68+ CD206+) was found to be increased in the presence of PNSECM within rodent sciatic defects (Figure 4A–B) as compared to conduit alone. The number of M1 macrophages was significantly increased in the PNSECM group at 2.5–3.0mm from the original site of transection ($p=0.01$, linear contrast) and M1 macrophages were identified up to 5.5mm from the original site of transection, in contrast to the control (3.5mm). The number of M2 macrophages was also significantly increased in the PNSECM group at each 500um interval from 1.0 to 3.0mm from the original site of transection (all $p=0.001$, linear contrast) and M1 macrophages were identified up to 5.5mm from the original site of transection, in contrast to the control (3.0mm). The presence of PNSECM also increased the M2:M1 ratio within the conduit ($p=0.002$, Figure 4C).

Schwann cells: Schwann cells (SC) tended to be distributed on the margins of the regenerative bridge and SC numbers were significantly increased in the PNSECM group at 2.5–3.0mm from the original site of transection ($p=0.02$, linear contrast). SC were identified up to 5.5mm from the original site of transection, in contrast to the control (3.5mm, Figure 4D).

Improvement of function with a common peroneal defect

As anticipated, modified peroneal functional index decreased significantly after injury in both control and PNSECM groups ($p<0.001$, figure 5). Partial recovery was observed in the PNSECM group with significantly improved PFI 8 and 16 weeks after nerve repair compared to the control group (linear contrasts $p=0.004$ and $p=0.006$ respectively). Overall

the interaction term (week * group) was significant (p=0.03) as were fixed effects for group (p=0.01) and week (p<0.001). Model fit was good (Adjusted R^2 =0.87) and model assumptions were met. We did not observe autophagy in any of the rats in either the short term (immunohistochemistrty) or long term (functional) studies.

DISCUSSION

In this study, we characterized the structure of an injectable peripheral nerve-specific ECM hydrogel, determined the biological effects of these hydrogels upon the early progression of peripheral nerve reconstruction across a critical gap defect, and demonstrated mild improvements in function using walking track analysis. We show that PNSECM hydrogels largely maintain matrix structure and several growth factors, promote increased macrophage invasion and higher percentages of M2 macrophages and enhance Schwann cell migration when transplanted into a rodent model.

ECM based scaffold materials such as those used in the present study have been derived from a wide variety of tissues and organs through decellularization. These materials have subsequently been used in a similarly wide variety of preclinical and clinical studies to promote constructive tissue remodeling at the implantation site. [31,45] The majority of the scaffold materials which are used clinically are derived from xenograft sources; however, a smaller number of decellularized tissue based products are sourced from cadaveric human tissues. In the present study, we chose to utilize a xenogeneic scaffold material composed of canine sciatic nerve. Canine tissue was utilized due to local availability, and the necessity of a large animal tissue source to provide sufficient tissue to complete the study. It is noted that the majority of the commercially available products utilize source tissues from porcine and bovine sources. Regardless of the tissue source, the development of effective decellularization protocols is essential to remove the majority of immunogenic cellular constituents while maintaining the tissue-specific structural and functional components intact. [37,46,47] For this reason, it is generally desirable to use the mildest, least disruptive protocol possible that yields an acellular material with the least interference to the structural and functional components of the ECM. The nerve-specific extracellular matrix generated by decellularization in the present study was demonstrated to be effectively decellularized with an 85% decrease in DNA content when compared to native tissue, yielding a material with similar or less DNA content than many commercially available ECM-based materials. [44]

The PNSECM used in this study retained many of the structural and functional components of native nerve following processing to remove cellular content. SEM demonstrated an ultrastructure similar to that of native nerve, with retention of predominantly the endoneurial architecture including the basal lamina. This was confirmed by immunofluorescent labeling that demonstrated preservation of large amounts of collagen IV, a component of the basal lamina. Previous studies have demonstrated that other tissues, such as UBM also maintains tissue-specific structural features including an intact basement membrane rich in collagen IV as well as the underlying submucosal connective tissues. [39] In the present study, a shift in the balance of hydroxyproline to GAG content was observed when comparing PNSECM and UBM. UBM likely contains an increased hydroxyproline content due to the maintenance of

the underlying submucosal tissues during decellularization, while the PNSECM processing involves stripping of the epineurium and scaffold materials are therefore enriched in non-fibrillar collagens and laminin, comparatively. Since the decellularization protocol was optimized to target immunogenic components such as cellular debris and myelin while maintaining the structural and functional proteins of the extracellular matrix, it is possible that the relative ratio of hydroxyproline and GAG to dry weight could remain the same or even to increase slightly because the decellularization protocol affected cellular components to a greater extent than these two structural proteins.

ECM hydrogels were found to be a practical solution for supporting nerve repair. The PNSECM degradation products begin to gel within 60 seconds after neutralizing to 7.4 pH at body temperature (37°C). The injectable substance was easy to handle and deliver to the site of injury. In a clinical setting, ECM hydrogels could be readily injected into an inert or bioactive conduit so that the liquid filled the available space before forming a hydrogel. Alternatively the hydrogel could be delivered directly at the site of nerve coaptation.

In the present study, when delivered into a rodent critically sized defect, we observed a switch in the ratio of M1:M2 phenotype macrophages, a phenomenon associated with improved nerve growth, [8] and promotion of Schwann cell migration across a gap defect. This was associated with improved function over time in a non-critical (8mm) common peroneal defect. We selected the common peroneal nerve as our experimental paradigm for functional studies as the consequence of axonal misdirection is reduced compared to sciatic nerve injury in which inappropriate reinnervation of muscular targets leads to dysfunction after injury . [48] We did not evaluate PNSECM in comparison to other biomaterials or biopolymers. This is the focus of ongoing work.

The present study does not attempt to investigate the mechanisms by which the injectable ECM promote these phenomena; however, a recent study has described M2 macrophage mediated angiogenesis as a mechanism leading to Schwann cell chemotaxis and downstream regeneration. [5] While ECM mediated shifts in macrophage phenotype have been reported in other applications, as has increased angiogenesis, further investigation of these phenomena in the context of nerve repair is warranted. Similarly, mechanistic studies linking these phenomena to improvements in function downstream should be performed. However, though the exact mechanisms are not clear, these results provide evidence that PNSECM is an effective tool for improving nerve repair.

5. CONCLUSION

In summary, here we characterize and show the effects of a nerve-specific extracellular matrix hydrogel on immunomodulation of the early macrophage response after nerve injury. We also describe effects on Schwann cell migration and function.

Acknowledgments

The authors would like to thank the Research in Animal Health Fund and the Harry M. Zweig Memorial Fund for Research for their support of this work (Cheetham, Cornell University). This work was financed in part by a grant from the Commonwealth of Pennsylvania through Innovation Works and through the support of the University of Pittsburgh, Office of Enterprise Development.

References

1. Chen D, Chen S, Wang W, Zhang C, Zheng H. Spontaneous regeneration of recurrent laryngeal nerve following long-term vocal fold paralysis in humans: Histologic evidence. Laryngoscope [Internet]. 2011; 121:1035–9. [cited 2013 Aug 4]; Available from: http://www.ncbi.nlm.nih.gov/pubmed/21520121.
2. Chiang F-YY, Wang L-FF, Huang Y-FF, Lee K-WW, Kuo W-RR. Recurrent laryngeal nerve palsy after thyroidectomy with routine identification of the recurrent laryngeal nerve. Surgery [Internet]. 2005; 137:342–7. [cited 2013 Aug 4]; Available from: http://www.ncbi.nlm.nih.gov/pubmed/15746790.
3. Daya H, Hosni A, Bejar-Solar I, Evans JN, Bailey CM. Pediatric vocal fold paralysis: a long-term retrospective study. Arch Otolaryngol Head Neck Surg [Internet]. 2000; 126:21–5. Available from: http://archotol.jamanetwork.com/article.aspx?doi=10.1001/archotol.126.1.21.
4. Woodson GE. Spontaneous laryngeal reinnervation after recurrent laryngeal or vagus nerve injury. Ann Otol Rhinol Laryngol [Internet]. 2007; 116:57–65. [cited 2016 May 23]; Available from: http://www.ncbi.nlm.nih.gov/pubmed/17305279.
5. Cattin A-L, Burden JJ, Van Emmenis L, Mackenzie FE, Hoving JJA, Garcia Calavia N, Guo Y, McLaughlin M, Rosenberg LH, Quereda V, Jamecna D, Napoli I, Parrinello S, Enver T, Ruhrberg C, Lloyd AC. Macrophage-Induced Blood Vessels Guide Schwann Cell-Mediated Regeneration of Peripheral Nerves. Cell [Internet]. 2015; 162:1127–39. [cited 2016 May 23]; Available from: http://www.pubmedcentral.nih.gov/articlerender.fcgi?artid=4553238&tool=pmcentrez&rendertype=abstract.
6. Khuong HT, Kumar R, Senjaya F, Grochmal J, Ivanovic A, Shakhbazau A, Forden J, Webb A, Biernaskie J, Midha R. Skin derived precursor Schwann cells improve behavioral recovery for acute and delayed nerve repair. Exp Neurol. 2014; 254:168–79. [PubMed: 24440805]
7. Lavasani M, Thompson SD, Pollett JB, Usas A, Lu A, Stolz DB, Clark KA, Sun B, Péault B, Huard J. Human muscle-derived stem/progenitor cells promote functional murine peripheral nerve regeneration. J Clin Invest [Internet]. 2014; 124:1745–56. Available from: http://www.jci.org/articles/view/44071.
8. Mokarram, N., Merchant, A., Mukhatyar, V., Patel, G., Bellamkonda, RV. Biomaterials [Internet]. Vol. 33. Elsevier Ltd; 2012. Effect of modulating macrophage phenotype on peripheral nerve repair; p. 8793-801.[cited 2013 Aug 4];Available from: http://www.ncbi.nlm.nih.gov/pubmed/22979988
9. Chen YY, McDonald D, Cheng C, Magnowski B, Durand J, Zochodne DW. Axon and Schwann cell partnership during nerve regrowth. J Neuropathol Exp Neurol [Internet]. 2005; 64:613–22. Available from: http://www.ncbi.nlm.nih.gov/pubmed/16042313.
10. Ghalib N, Houst'ava L, Haninec P, Dubovy P. Morphometric analysis of early regeneration of motor axons through motor and cutaneous nerve grafts. Ann Anat. 2001; 183:363–8. [PubMed: 11508363]
11. Hall SM. Regeneration in cellular and acellular autografts in the peripheral nervous system. Neuropathol Appl Neurobiol. 1986; 12:27–46. [PubMed: 3703154]
12. Hall SM. The effect of inhibiting Schwann cell mitosis on the re-innervation of acellular autografts in the peripheral nervous system of the mouse. Neuropathol Appl Neurobiol. 1986; 12:401–14. [PubMed: 3095674]
13. Hall SM. Regeneration in the peripheral nervous system. Neuropathol Appl Neurobiol. 1989; 15:513–29. [PubMed: 2693992]
14. Mills CD, Kincaid K, Alt JM, Heilman MJ, Hill AM. M-1/M-2 Macrophages and the Th1/Th2 Paradigm. J Immunol [Internet]. 2000; 164:6166–73. Available from: http://www.jimmunol.org/cgi/doi/10.4049/jimmunol.164.12.6166.
15. Gordon S. Alternative activation of macrophages. Nat Rev Immunol [Internet]. 2003; 3:23–35. [cited 2013 Aug 1]; Available from: http://www.ncbi.nlm.nih.gov/pubmed/12511873.
16. Mantovani, A., Sica, A., Sozzani, S., Allavena, P., Vecchi, A., Locati, M. Centro di Eccellenza per l'Innovazione Diagnostica e Terapeutica (IDET). Vol. 25. Institute of General Pathology, University of Milan; I-20133 Milan, Italy: Istituto di Ricerche Farmacologiche Mario Negri; I-20157 Milan, Italy: 2004. The chemokine system in diverse forms of macrophage activation and

polarization. Trends Immunol [Internet]; p. 677-86.[cited 2013 Jul 31];Available from: http://www.ncbi.nlm.nih.gov/pubmed/15530839

17. Terris DJ, Toft KM, Moir M, Lum J, Wang M. Brain-derived neurotrophic factor-enriched collagen tubule as a substitute for autologous nerve grafts. Arch Otolaryngol Head Neck Surg [Internet]. 2001; 127:294–8. [cited 2016 May 23]; Available from: http://www.ncbi.nlm.nih.gov/pubmed/11255474.
18. Wood, MD., Moore, AM., Hunter, DA., Tuffaha, S., Borschel, GH., Mackinnon, SE., Sakiyama-Elbert, SE. Acta Biomater [Internet]. Vol. 5. Acta Materialia Inc; 2009. Affinity-based release of glial-derived neurotrophic factor from fibrin matrices enhances sciatic nerve regeneration; p. 959-68.[cited 2013 Aug 4];Available from: http://dx.doi.org/10.1016/j.actbio.2008.11.008
19. Fine EG, Decosterd I, Papaloizos M, Zurn AD, Aebischer P, Papaloïzos M, Zurn AD, Aebischer P. GDNF and NGF released by synthetic guidance channels support sciatic nerve regeneration across a long gap. Eur J Neurosci [Internet]. 2002; 15:589–601. Available from: http://www.ncbi.nlm.nih.gov/pubmed/11886440.
20. Moore AM, Wood MD, Chenard K, Hunter DA, Mackinnon SE, Sakiyama-Elbert SE, Borschel GH. Controlled delivery of glial cell line-derived neurotrophic factor enhances motor nerve regeneration. J Hand Surg Am [Internet]. 2010; 35:2008–17. [cited 2016 May 23]; Available from: http://www.ncbi.nlm.nih.gov/pubmed/21035963.
21. Lee AC, Yu VM, Lowe JB, Brenner MJ, Hunter DA, Mackinnon SE, Sakiyama-Elbert SE. Controlled release of nerve growth factor enhances sciatic nerve regeneration. Exp Neurol [Internet]. 2003; 184:295–303. [cited 2016 May 23]; Available from: http://www.ncbi.nlm.nih.gov/pubmed/14637100.
22. Dodla MC, Bellamkonda RV. Differences between the effect of anisotropic and isotropic laminin and nerve growth factor presenting scaffolds on nerve regeneration across long peripheral nerve gaps. Biomaterials [Internet]. 2008; 29:33–46. [cited 2013 Aug 4]; Available from: http://www.pubmedcentral.nih.gov/articlerender.fcgi?artid=2682535&tool=pmcentrez&rendertype=abstract.
23. Midha R, Munro CA, Dalton PD, Tator CH, Shoichet MS. Growth factor enhancement of peripheral nerve regeneration through a novel synthetic hydrogel tube. J Neurosurg [Internet]. 2003; 99:555–65. [cited 2016 May 23]; Available from: http://www.ncbi.nlm.nih.gov/pubmed/12959445.
24. Mimura T, Dezawa M, Kanno H, Sawada H, Yamamoto I. Peripheral nerve regeneration by transplantation of bone marrow stromal cell-derived Schwann cells in adult rats. J Neurosurg [Internet]. 2004; 101:806–12. Available from: http://www.ncbi.nlm.nih.gov/pubmed/15540919.
25. Mosahebi A, Wiberg M, Terenghi G. Addition of fibronectin to alginate matrix improves peripheral nerve regeneration in tissue-engineered conduits. Tissue Eng [Internet]. 2003; 9:209–18. [cited 2016 May 23]; Available from: http://www.ncbi.nlm.nih.gov/pubmed/12740084.
26. Hsu S-H, Chang C-J, Tang C-M, Lin F-T. In vitro and in vivo effects of Ginkgo biloba extract EGb 761 on seeded Schwann cells within poly(DL-lactic acid-co-glycolic acid) conduits for peripheral nerve regeneration. J Biomater Appl [Internet]. 2004; 19:163–82. [cited 2016 May 23]; Available from: http://www.ncbi.nlm.nih.gov/pubmed/15381788.
27. Udina E, Rodríguez FJ, Verdú E, Espejo M, Gold BG, Navarro X. FK506 enhances regeneration of axons across long peripheral nerve gaps repaired with collagen guides seeded with allogeneic Schwann cells. Glia [Internet]. 2004; 47:120–9. [cited 2016 May 23]; Available from: http://www.ncbi.nlm.nih.gov/pubmed/15185391.
28. Sierpinski P, Garrett J, Ma J, Apel P, Klorig D, Smith T, Koman LA, Atala A, Van Dyke M. The use of keratin biomaterials derived from human hair for the promotion of rapid regeneration of peripheral nerves. Biomaterials [Internet]. 2008; 29:118–28. [cited 2016 May 23]; Available from: http://www.ncbi.nlm.nih.gov/pubmed/17919720.
29. Apel PJ, Garrett JP, Sierpinski P, Ma J, Atala A, Smith TL, Koman LA, Van Dyke ME. Peripheral nerve regeneration using a keratin-based scaffold: long-term functional and histological outcomes in a mouse model. J Hand Surg Am [Internet]. 2008; 33:1541–7. [cited 2016 May 23]; Available from: http://www.ncbi.nlm.nih.gov/pubmed/18984336.
30. Hoben G, Yan Y, Iyer N, Newton P, Hunter DA, Moore AM, Sakiyama-Elbert SE, Wood MD, Mackinnon SE. Comparison of acellular nerve allograft modification with Schwann cells or

VEGF. Hand (N Y) [Internet]. 2015; 10:396–402. [cited 2016 May 23]; Available from: http://www.ncbi.nlm.nih.gov/pubmed/26330769.

31. Brown BN, Badylak SF. Extracellular matrix as an inductive scaffold for functional tissue reconstruction. Transl Res [Internet]. 2014; 163:268–85. Available from: http://dx.doi.org/10.1016/j.trsl.2013.11.003.
32. Agrawal V, Brown BN, Beattie AJ, Gilbert TW, Badylak SF. Evidence of innervation following extracellular matrix scaffold-mediated remodelling of muscular tissues. J Tissue Eng Regen Med. 2009; 3:590–600. [PubMed: 19701935]
33. Turner NJ, Yates AJ, Weber DJ, Qureshi IR, Stolz DB, Gilbert TW, Badylak SF. Xenogeneic extracellular matrix as an inductive scaffold for regeneration of a functioning musculotendinous junction. Tissue Eng Part A [Internet]. 2010; 16:3309–17. Available from: http://www.ncbi.nlm.nih.gov/pubmed/20528669.
34. Valentin JE, Turner NJ, Gilbert TW, Badylak SF. Functional skeletal muscle formation with a biologic scaffold. Biomaterials [Internet]. 2010; 31:7475–84. Available from: http://www.ncbi.nlm.nih.gov/pubmed/20638716.
35. Agrawal V, Tottey S, Johnson Sa, Freund JM, Siu BF, Badylak SF. Recruitment of Progenitor Cells by an Extracellular Matrix Cryptic Peptide in a Mouse Model of Digit Amputation. Tissue Eng Part A. 2011; 17:2435–43. [PubMed: 21563860]
36. Freytes DO, Martin J, Velankar SS, Lee AS, Badylak SF. Preparation and rheological characterization of a gel form of the porcine urinary bladder matrix. Biomaterials [Internet]. 2008; 29:1630–7. Available from: http://www.ncbi.nlm.nih.gov/pubmed/18201760.
37. Medberry CJ, Crapo PM, Siu BF, Carruthers CA, Wolf MT, Nagarkar SP, Agrawal V, Jones KE, Kelly J, Johnson SA, Velankar SS, Watkins SC, Modo M, Badylak SF. Hydrogels derived from central nervous system extracellular matrix. Biomaterials [Internet]. 2013; 34:1033–40. [cited 2016 May 23]; Available from: http://www.pubmedcentral.nih.gov/articlerender.fcgi?artid=3512573&tool=pmcentrez&rendertype=abstract.
38. Crapo PM, Medberry CJ, Reing JE, Tottey S, van der Merwe Y, Jones KE, Badylak SF. Biologic scaffolds composed of central nervous system extracellular matrix. Biomaterials [Internet]. 2012; 33:3539–47. [cited 2016 Mar 23]; Available from: http://www.pubmedcentral.nih.gov/articlerender.fcgi?artid=3516286&tool=pmcentrez&rendertype=abstract.
39. Brown B, Lindberg K, Reing J, Stolz DB, Badylak SF. The basement membrane component of biologic scaffolds derived from extracellular matrix. Tissue Eng [Internet]. 2006; 12:519–26. [cited 2016 May 23]; Available from: http://www.ncbi.nlm.nih.gov/pubmed/16579685.
40. Kilkenny C, Browne WJ, Cuthill IC, Emerson M, Altman DG. Improving Bioscience Research Reporting: The ARRIVE Guidelines for Reporting Animal Research. PLoS Biol [Internet]. 2010; 8:e1000412. Available from: http://dx.plos.org/10.1371/journal.pbio.1000412.
41. Lundborg G, Dahlin LB, Danielsen N, Gelberman RH, Longo FM, Powell HC, Varon S. Nerve regeneration in silicone chambers: influence of gap length and of distal stump components. Exp Neurol [Internet]. 1982; 76:361–75. Available from: http://www.ncbi.nlm.nih.gov/pubmed/7095058.
42. Bain JR, Mackinnon SE, Hunter DA. Functional evaluation of complete sciatic, peroneal, and posterior tibial nerve lesions in the rat. Plast Reconstr Surg [Internet]. 1989; 83:129–38. [cited 2015 Dec 9]; Available from: http://www.ncbi.nlm.nih.gov/pubmed/2909054.
43. GrandPré T, Li S, Strittmatter SM. Nogo-66 receptor antagonist peptide promotes axonal regeneration. Nature [Internet]. 2002; 417:547–51. [cited 2016 May 23]; Available from: http://www.ncbi.nlm.nih.gov/pubmed/12037567.
44. Gilbert TW, Freund JM, Badylak SF. Quantification of DNA in biologic scaffold materials. J Surg Res [Internet]. 2009; 152:135–9. [cited 2016 May 23]; Available from: http://www.pubmedcentral.nih.gov/articlerender.fcgi?artid=2783373&tool=pmcentrez&rendertype=abstract.
45. Badylak SF, Brown BN, Gilbert TW, Daly KA, Huber A, Turner NJ. Biologic scaffolds for constructive tissue remodeling. Biomaterials [Internet]. 2011; 32:316–9. [cited 2016 May 23]; Available from: http://www.ncbi.nlm.nih.gov/pubmed/21125721.

46. Brown, BN., Valentin, JE., Stewart-Akers, AM., McCabe, GP., Badylak, SF. Biomaterials [Internet]. Vol. 30. Elsevier Ltd; 2009. Macrophage phenotype and remodeling outcomes in response to biologic scaffolds with and without a cellular component; p. 1482-91.[cited 2013 Aug 4];Available from: http://www.pubmedcentral.nih.gov/articlerender.fcgi?artid=2805023&tool=pmcentrez&rendertype=abstract

47. Meng F, Modo M, Badylak SF. Biologic scaffold for CNS repair. Regen Med [Internet]. 2014; 9:367–83. [cited 2016 May 23]; Available from: http://www.ncbi.nlm.nih.gov/pubmed/24935046.

48. Wood, MD., Kemp, SWP., Weber, C., Borschel, GH., Gordon, T. Ann Anat [Internet]. Vol. 193. Elsevier GmbH; 2011. Outcome measures of peripheral nerve regeneration; p. 321-33.[cited 2013 Aug 4];Available from: http://dx.doi.org/10.1016/j.aanat.2011.04.008

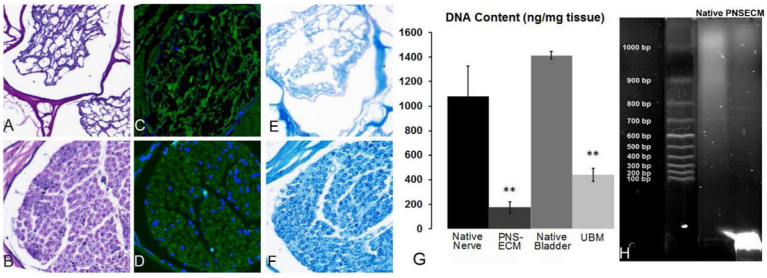

Figure 1.

Qualitative assessment of decellularization. Decellularized canine sciatic nerve shows significantremoval of nuclei through H&E staining (A) compared to native sciatic tissue (B). Dapi stain in decellularized (C) and native (D) shows similar results with a small number of disrupted nuclei remaining. Luxol Fast Blue staining myelin dark blue is reduced after decellularization (E) within the endoneurial tissue compared to dark circles of myelin in native tissue (F). (G) Picogreen assay for DNA content shows dsDNA content of the decellularized tissue of both PNSECM and urinary bladder matrix was significantly decreased as compared to native tissues (**, $p<0.05$, $n=5$). (H) The dsDNA that remains within PNSECM was highly fragmented (<100bp) compared to dsDNA extracted from native tissue.

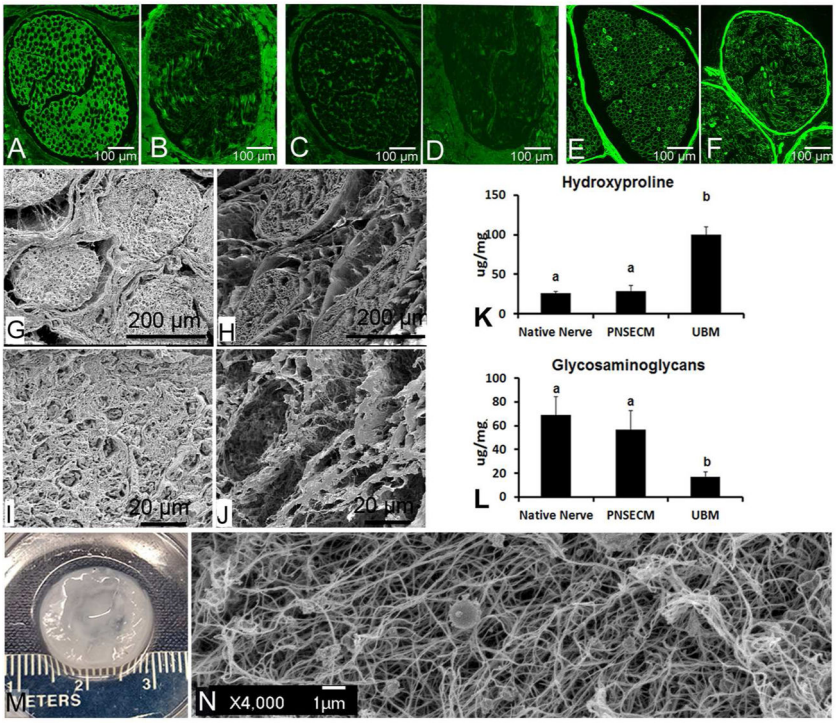

Figure 2.

Characterization of remaining content within canine sciatic nerve after decellularization. (A–F) Immunofluorescent staining of collagen I, collagen III, and collagen IV before and after decellularization Collagen I was seen both within the endoneurial and epineurial space before decellularization (A) but was reduced by decellularization (B). Little positive staining of collagen III was seen in both native (C) and decellularized (D) sciatic nerve tissue sections. Collagen IV, a major component of the basal lamina had strong staining around the individual nerve fibers, in the endoneurial space, and in the perineurium in native nerve (E). The same pattern of collagen IV staining was seen in the decellularized nerve tissue (F) suggesting a preservation of the basal lamina. (G, H) Low and (I, J) high magnification scanning electron microscopy (SEM) images of native and decellularized sciatic nerve. Cross-sectioned native (G) and decellularized (H) tissue at 150X magnification shows a dense epineurial space that it is largely cleared by decellularization but perineurium and endoneurium structure largely maintained. Enhanced magnification (1000X) of the same samples, native (I) and decellularized (J) endoneurial tissue. Images show the presence (I) and removal of (J) axons within the endonerium. Biochemical assays for hydroxyproline (K) and glycosaminoglycans (GAG) (L) did not reveal any significant changes to either component after peripheral nerve decellularization ($p=0.57$ $n=5$, $p=0.26$ $n=5$). These components were compared to urinary bladder matrix (UBM) which had significantly more hydroxylproline but significantly less GAG than PNSECM and native nerve. Different letters denote a significant difference ($p<0.05$).Image shows macroscopic (E) and SEM image (F) of an 8 mg/ml equine PNS-ECM hydrogel

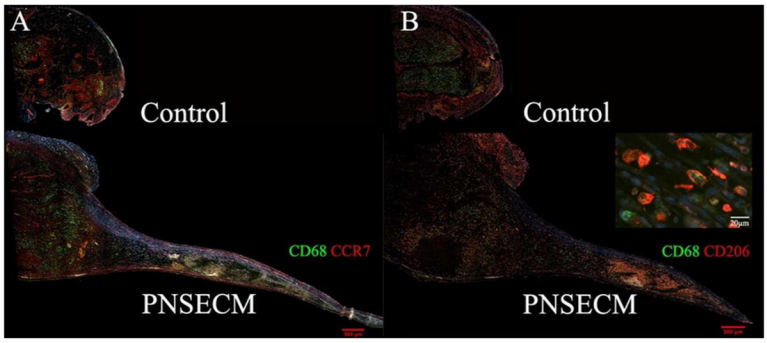

Figure 3.

Representative longitudinal sections of regenerative bridges immunohistolabeled for M1 macrophages (panel A, CD68+CCR7+) for control (empty conduit) and PNSECM filled conduits. Representative immunolabeling for M2 (panel B, CD68+CD206+) macrophages in empty and PNSECM filled conduits. Insert demonstrates intracellular CD 68 labelling and surface CD206 labelling. No additional extension of proximal stump was observed in control sections.

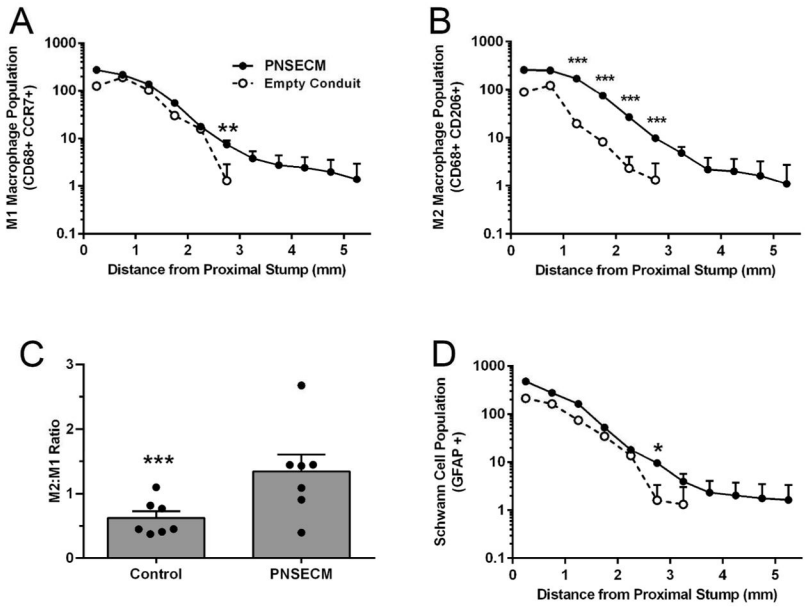

Figure 4.

PNSECM promotes migration of both M1 (CD68+CCR7+) and M2 (CD68+CD206+) macrophage phenotypes, relative to the original site of transection (A,B); an increased M2:M1 ratio (C) and increased extension of Schwann cells populations relative to the original site of transection (D). Data shown are least square (adjusted) mean and standard error (A,B,D) and mean and standard error (C). n= 3 slides/ label/animal and 7 animals / group.

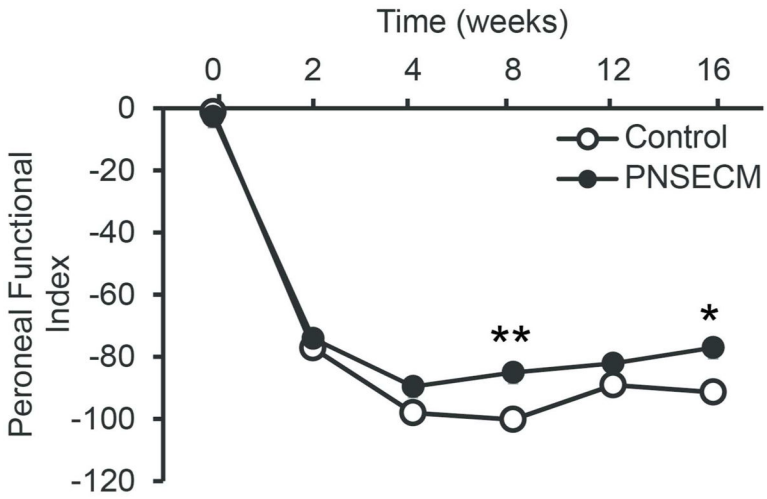

Figure 5.

PNSECM improves hind limb function determined by walking track analysis and modified peroneal functional index. PFI was significantly higher in the PNSECM group 8 and 16 weeks after nerve repair compared to the control group (linear contrasts p=0.004 and p=0.006 respectively, n=6 / group).

Table 1

Growth Factor/Cell	Matrix	Conduit material	Animal model	Conclusions	Ref
BDNF	Collagen	Collagen	Rabbit facial nerve; 15 mm, n=10	BDNF did not appear to promote better regeneration than collagen matrix only.	(Terris et al. 2001)
GDNF	Fibrin	Silicone	Rat sciatic nerve; 13 mm, n=12	GDNF delivery system generated significantly less nerve fibers at middle line of conduit than isograft but fibers were more mature.	(Wood et al. 2009)
	EVA/BSA	EVA	Rat sciatic nerve; 15 mm, n=10	GDNF promoted approximately 20% and 35% regeneration of motor and sensory neurons respectively.	(Fine et al. 2002)
	Fibrin	Silicone	Rat femoral nerve; 5 mm, n=7	Controlled delivery of GDNF led to enhanced nerve regeneration that was not significantly different then isograft control.	(Moore et al. 2010)
NGF	Fibrin	Silicone	Rat sciatic nerve; 13 mm, n=6	NGF was not significantly different from the isograft control including showing similar nerve maturity and density.	(Lee et al. 2003)
	EVA/BSA	EVA	Rat sciatic nerve; 15 mm, n=10	Only 5% of the total number of motor and sensory neurons regenerated with treatment of NGF after 6 weeks.	(Fine et al. 2002)
NT-3	Collagen	PHEMA- MMA	Rat sciatic nerve; 10mm, n=6	The introduction of a high dose of fibroblast growth factor (FBF-1) was comparable to isograft and was significantly better than NT-3, BDNF, and matrix alone.	(Rajiv Midha et al. 2003)
Schwann Cells	Collagen	PLGA	Rat sciatic nerve; 12 mm, n=9	The bone marrow stromal cell derived Schwann cells produced better histologic and functional outcomes than matrix alone but did not match autograft control.	(Mimura et al. 2004)
	Alginate/fibronectin	PHB	Rat sciatic nerve; 10 mm, n=6	Transplanted Schwann cells and fibronectin had an additive effect on regeneration over negative controls.	(Mosahebi, Wiberg, and Terenghi 2003)
	Gelatin	PLGA	Rat sciatic nerve; 10 mm, n=6	The addition of Ginkgo biloba extract with Schwann cells increased motor unit action potential at 6 weeks after injury over autograft control.	(Hsu et al. 2004)
	Matrigel	Collagen	Mouse sciatic nerve 6 mm, n=9	Allogeneic Schwann cells did not provide a benefit over matrix only control but the addition of FK506, an immunosuppressant improved results over negative control.	(Udina et al. 2008)
Matrix Alone	Keratin	Silastic	Mouse tibial nerve; 4 mm, n=5	Keratin increase histologic and electophysiologic measures of recovery over autograft, however these results did not translate to muscle function recovery after 6 weeks.	(Sierpinski et al. 2008)
	Keratin	Silicone	Mouse tibial nerve 5 mm, n=6	Keratin hydrogel improved eletrophysiologic and histologic measurement of recovery over empty conduits and autograft controls.	(Apel et al. 2008)

Author Manuscript

Author Manuscript

Author Manuscript

Table 2

Antibody	Host species	Isotype	Dilution	Source
CD206 (C-20)	goat	IgG, polyclonal	1:50	Santa Cruz
CCR7 (Y59)	rabbit	IgG, monoclonal	1:500	Abcam
CD68 (ED1)	mouse	IgG1, monoclonal	1:50	BioRad
GFAP	rabbit	IgG, whole antiserum	1:500	Abcam
NF200	mouse	IgG1, monoclonal	1:50	Abcam